ELSEVIER

Polymer 40 (1999) 6529–6538

polymer

Hard segmented side chain liquid crystal polyurethanes with azobenzene mesogenic moieties

Marko Brecl*, Majda Žigon

National Institute of Chemistry, Hajdrihova 19, SI-1000 Ljubljana, Slovenia

Received 10 September 1998; received in revised form 8 December 1998; accepted 8 December 1998

Abstract

A series of side chain liquid crystal polyurethanes (C*n*OMeP) with even-numbers of methylene units in the spacer was synthesised by the addition polymerisation of α-[bis(2-hydroxyethyl)amino]-ω-(4-methoxyazobenzene-4′-oxy)alkanes (C*n*OMe-diol) with hexamethylene diisocyanate. The thermal and structural properties of C*n*OMeP were determined by means of polarising optical microscopy (POM), differential scanning calorimetry (DSC) and X-ray diffraction. C2- and C4OMeP showed a completely amorphous nature, while C6–C12OMeP exhibited a bilayer smectic structure. Polyurethane backbones have a high tendency to crystallise. Crystallisation is closely related to hydrogen bonding between polyurethane groups. Short spacers favour an amorphous nature, while longer ones tend to lead to crystallisation. In order to obtain further information concerning backbone crystallisation, Fourier transform infrared spectroscopy (FT-IR) studies of C*n*OMeP polyurethanes were carried out at different temperatures focusing on the H-bonds between the N–H and C=O groups of the polyurethane backbone.

Keywords: Mesomorphic side chain polyurethanes; Bilayer smectic phases; H-bonds

1. Introduction

As the first liquid crystal polymers were synthesised, their chemical structure–property correlations were investigated extensively. In particular, liquid crystal polymers have promising potential applications ranging from the production of high strength fibres (main chain liquid crystal polymers) to their use in optical devices (side chain liquid crystal polymers) [1–3]. By varying individual structural parts (in the case of side chain liquid crystal polymers, the polymer backbone, the spacer and mesogenic unit), polymer molar mass, polydispersity and tacticity, liquid crystal behaviour can be successfully controlled [4–10]. Some general qualitative rules on how the above mentioned individual variables influence the liquid crystalline properties were determined. For instance, in side chain liquid crystal polymers, glass transition temperatures decrease with increasing spacer length, short spacers tend to lead to nematic phases, while longer ones favour smectic phases. These general rules have been widely discussed in the literature [11–13]. Nevertheless, although the qualitative rules are well established, it is impossible to predict any detailed quantitative information concerning the mesomorphic behaviour of newly synthesised mesomorphic polymers.

Side chain liquid crystal polyurethanes have not been investigated extensively, at least not as systematically as side chain liquid crystal polymers with acrylic, methacrylic and siloxane backbones [14]. To our knowledge the first two series of side chain liquid crystal polyuretanes with spacer lengths varying from 2 to 12 methylene groups have been published only recently [15,16].

This article reports on the synthesis and the mesomorphic properties of hard segmented side chain liquid crystal polyurethanes (C*n*OMeP) containing methoxyazobenzene mesogenic units prepared by the addition polymerisation of α-[bis(2-hydroxyethyl)amino]-ω-(4-methoxyazobenzene-4′-oxy)alkanes (C*n*OMe-diol) with hexamethylene diisocyanate (HDI).

2. Experimental

2.1. The synthesis of monomers (CnOMe-diol) and the corresponding polyurethanes (CnOMeP) (Scheme 1)

2.1.1. Monomers (CnOMe-diols)

α-[Bis(2-hydroxyethyl)amino]-ω-(4-methoxyazobenzene-4′-oxy)alkanes (C*n*OMe-diols) were synthesised according to the procedure described in our previous papers

* Corresponding author.

0032-3861/99/$ - see front matter
PII: S0032-3861(98)00844-1

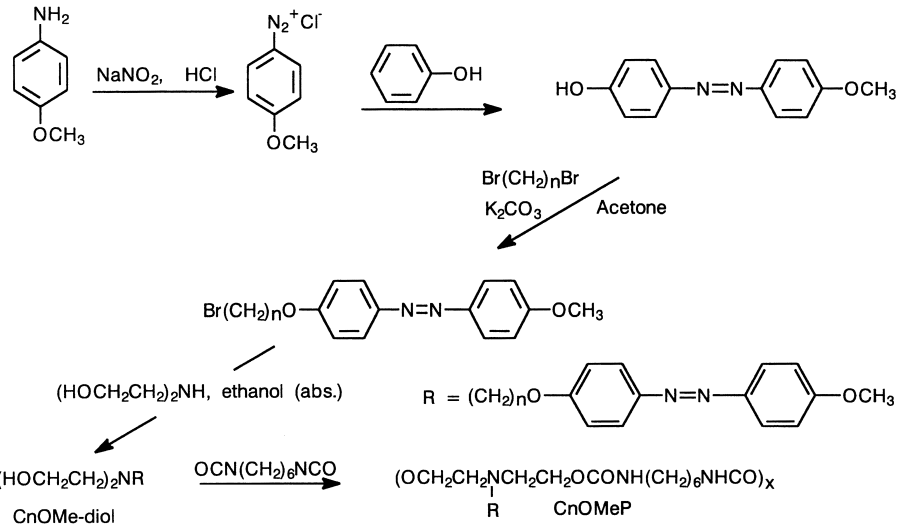

Scheme 1.

on the synthesis of α-[bis(2-hydroxyethyl)amino]-ω-(4-cyanoazobenzene-4′-oxy)alkanes and α-[bis(2-hydroxyethyl)amino]-ω-(4-nitroazobenzene-4′-oxy)alkanes, respectively [15–17]. α-[Bis(2-hydroxyethyl)amino]-ω-(4-methoxyazobenzene-4′-oxy)alkanes are denoted as C*n*OMe-diols. *n* is the number of methylene units in the alkyl chain ($n = 2$, 4, 6, 8, 10 and 12). Scheme 1 shows the sequence of reactions leading to C*n*OMe-diols and corresponding polyurethanes (C*n*OMeP). The structure of the synthesised diols was confirmed by elemental analysis (Table 1), NMR spectroscopy and FTIR spectroscopy.

^{1}H-NMR spectra of C*n*OMe-diols (300 MHz, $CDCl_3$, TMS, 25°C, δ (ppm), *J* (Hz))

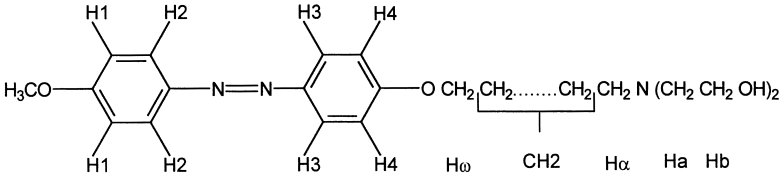

The chemical shifts and coupling constants of the aromatic protons (H1–H4) are the same for all C*n*OMe-diols, while those of alkyl chains are basically the same as of α-[bis(2-hydroxyethyl)amino]-ω-(4-cyanoazobenzene-4′-oxy)alkanes and α-[bis(2-hydroxyethyl)amino]-ω-(4-nitroazobenzene-4′-oxy)alkanes, published in our previous papers [15,16]. Therefore, they are given for the representative example of C10OMe-diol only.

C10OMe-diol. δ: 7.85 (crossed doublets, 4H, *J* 9.0 Hz, H1, H4), 7.01 (crossed doublets, 4H, *J* 9.0 Hz, H2, H3), 4.02 (t, 2H, *J* 6.5 Hz, Hω), 3.88 (s, 3H, OCH_3), 3.61 (t, 4H, *J* 5.4 Hz, Hb), 2.79 (bs, 2H, OH), 2.65 (t, 4H, *J* 5.4 Hz, Ha), 2.51 (t, 2H, *J* 7.4 Hz, Hα), 1.80 (p, 2H, *J* 7.0 Hz, CH2), 1.22–1.54 (mp, 14H, CH2).

2.1.2. Polyurethanes (CnOMeP)

C*n*OMe-diols were polymerised by addition polymerisation with hexamethylene diisocyanate (HDI) to corresponding C*n*OMeP polyurethanes. C*n*OMe-diol (0.002 mol), hexamethylene diisocyanate (0.002 mol), DMF (10 ml) as a solvent, and dibutyltin dilaurate (0.2% with respect to the

Table 1
Elemental analysis of α-[bis(2-hydroxyethyl)amino]-ω-(4-methoxyazobenzene-4′-oxy)alkanes (C*n*OMe-diols)

n	Formula	Mol. wt.	%C		%H		%N	
			Calc.	Found	Calc.	Found	Calc.	Found
2	$C_{19}H_{25}N_3O_4$	359.42	63.49	63.65	7.01	7.27	11.69	11.85
4	$C_{21}H_{29}N_3O_4$	387.48	65.10	65.17	7.54	7.81	10.84	10.97
6	$C_{23}H_{33}N_3O_4$	415.53	66.48	66.68	8.00	8.45	10.11	10.11
8	$C_{25}H_{37}N_3O_4$	443.59	67.69	67.66	8.41	8.71	9.47	9.59
10	$C_{27}H_{41}N_3O_4$	471.64	68.76	68.75	8.76	9.11	8.91	9.00
12	$C_{29}H_{45}N_3O_4$	499.69	69.71	69.71	9.08	9.41	8.41	8.58

Table 2
Elemental analysis, weight-average molar masses ($\overline{M}_w$) and polydispersities ($\overline{M}_w/\overline{M}_n$) of C*n*OMeP polyurethanes

n	Formula	Mol. wt.	%C		%H		%N		$\overline{M}_w \times 10^{-3}$(g/mol)	$\overline{M}_w/\overline{M}_n$
			Calc.	Found	Calc.	Found.	Calc.	Found		
2	$(C_{27}H_{37}N_5O_6)_x$	$(527.62)_x$	61.46	61.33	7.07	7.35	13.27	13.18	106	3.8
4	$(C_{29}H_{41}N_5O_6)_x$	$(555.67)_x$	62.68	62.62	7.44	7.80	12.60	12.50	57	3.0
6	$(C_{31}H_{45}N_5O_6)_x$	$(583.73)_x$	63.79	63.35	7.77	8.13	12.05	11.93	24	3.2
8	$(C_{33}H_{49}N_5O_6)_x$	$(611.78)_x$	64.79	64.41	8.07	8.41	11.45	11.38	44	3.9
10	$(C_{35}H_{53}N_5O_6)_x$	$(639.83)_x$	65.70	65.44	8.35	8.77	10.95	10.79	44	3.9
12	$(C_{37}H_{57}N_5O_6)_x$	$(667.89)_x$	66.54	66.26	8.60	9.02	10.49	10.38	32	3.5

diol) as catalyst were placed into a 50 ml round-bottomed flask. All the reagents as well as the solvent were weighed in a dry box to avoid water contamination. The reaction mixture was stirred by a magnetic stirrer at 70°C for 3 h. Polyurethanes were precipitated in ethanol, purified by dissolution in DMF and reprecipitation in ethanol, subsequently they were air-dried. Polyurethanes were denoted as C*n*OMeP (Scheme 1), where *n* is the number of methylene units in the spacer. Their composition was examined by elemental analysis (Table 2). Weight-average molar masses ($\overline{M}_w$) and polydispersities ($\overline{M}_w/\overline{M}_n$) as measured by size-exclusion chromatography (SEC) are given in Table 2.

2.2. Characterisation methods

2.2.1. NMR spectroscopy

The ^{1}H-NMR spectra were recorded at 25°C on a Varian VXR 300 spectrometer at 300 MHz using TMS as an internal standard. $CDCl_3$ was used as a solvent. Pulse length: 9.9 ms, acquisition time: 3.75 s, delay time: 2.0 s, number of scans: 32.

2.2.2. Elemental analysis

Elemental analyses were carried out on a Perkin–Elmer analyser, model 240 C.

2.2.3. Size-exclusion chromatography

Average molar masses and molar mass distributions were determined by SEC on a modular Perkin–Elmer liquid chromatograph equipped with a UV detector. A precolumn, a PL gel column Mixed C (30 cm × 7 mm, particle size 4–5 μm with a linear working range of molar masses between 500 and 5×10^6 g/mol, Polymer Laboratories) and THF as an eluent (1 ml/min) were used. The calibration was performed with polystyrene standards (Toyo Soda Manufacturing) in the molar mass region of 500–3.7×10^6 g/mol.

2.2.4. Differential scanning calorimetry

Thermal characterisation was carried out by a Perkin–Elmer DSC 7 differential scanning calorimeter. The given values of T_g, transition temperatures and corresponding enthalpies, were average values of at least two measurements taken at the second heating and cooling cycle, respectively. All samples were treated in the same way. Each sample was placed into a DSC heating cell at 50°C, cooled to −50°C, maintained at −50°C for 3 min, heated to 150°C, maintained at 150°C for 3 min, cooled to −50°C, maintained at −50°C for 3 min and reheated once again. The scanning rate was 10 K/min.

2.2.5. Polarising optical microscopy

Optical textures were obtained by using a Carl Zeiss polarising optical microscope Stemi SV6 equipped with a microscope camera MC 80 and a Mettler Toledo FP82 hot stage. The sample was pressed between a glass slide and cover slip and observed in the LC-temperature range.

2.2.6. Fourier transform infrared spectroscopy

Infrared spectra at various temperatures were obtained by a Perkin–Elmer FT-IR 1725 X spectrophotometer equipped with a Spectra-Tech heating cell. The resolution was 4 cm^{-1}. The sample was pressed between two NaCl crystal plates and heated to the desired temperature in the heating cell.

2.2.7. X-ray diffraction

X-ray diffraction patterns were taken on a Siemens D-5000 diffractometer using CuK_α radiation ($\lambda = 1.54$ Å) in 0.02° steps from 1°–30° (in 2θ) with 20 s (Figs. 5 and 6) or 2 s (Fig. 4) per step. X-ray measurements were carried out

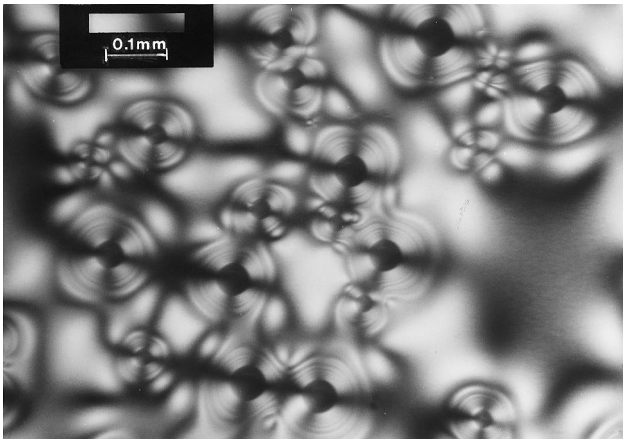

Fig. 1. The schlieren texture of C8OMeP polyurethane obtained on fast cooling of the isotropic phase.

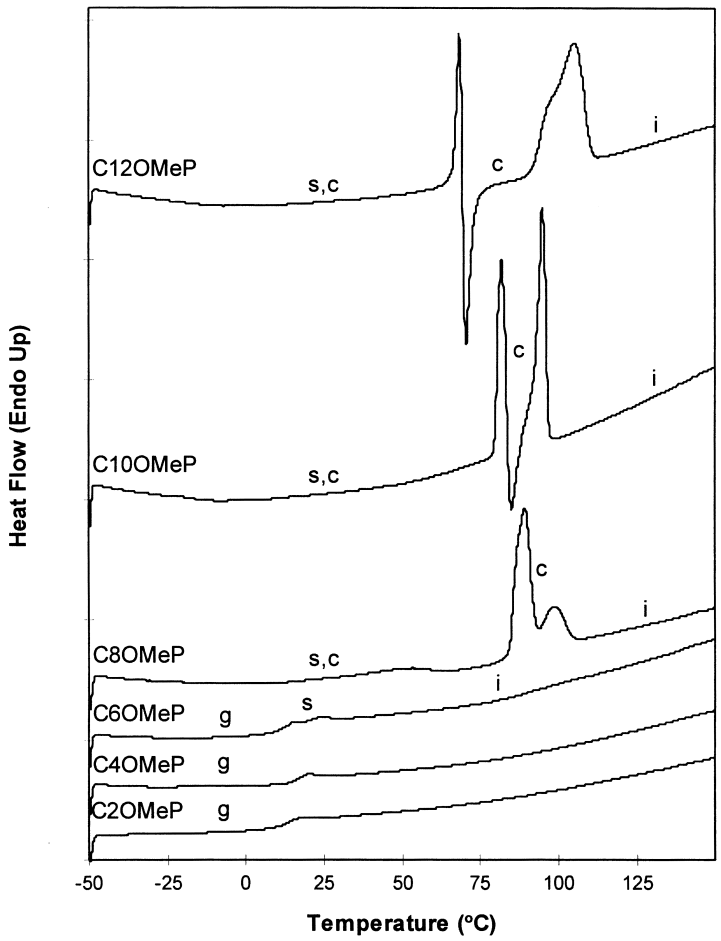

Fig. 2. The normalised second heating DSC scans of C*n*OMeP polyurethanes (10°C min^{-1}): g – glassy phase, s – smectic phase, c – crystal phase, i – isotropic phase.

on free-standing unoriented films approximately 0.5 mm thick prepared by moulding the polymers at 150°C.

3. Results and discussions

The liquid crystalline properties of C*n*OMePs were determined by means of differential scanning calorimetry, polarising optical microscopy (POM) and X-ray diffraction. Fig. 1 shows an optical texture of C8OMeP, which is a combination of a schlieren texture and an arced focal-conic-texture. The texture was obtained on fast cooling of the isotropic phase. The rapid cooling was important in order to prevent crystallisation. A similar optical texture was observed for C6OMeP, but the texture was not as clear as that obtained for C8OMeP polyurethane. However, we were not able to obtain clear optical textures for C10- and C12OMeP because of their high tendency toward crystallisation.

Fig. 2 shows the second heating DSC scans of C*n*OMeP polyurethanes. C2- and C4OMeP exhibit a glass transition at 12°C ($\Delta C_p = 0.65\ \mathrm{J\,g^{-1}\,K^{-1}}$) and 17°C ($\Delta C_p = 0.60\ \mathrm{J\,g^{-1}\,K^{-1}}$) respectively, because of their amorphous nature. A DSC scan of C6OMeP shows a glass transition at 12°C ($\Delta C_p = 0.70\ \mathrm{J\,g^{-1}\,K^{-1}}$) followed by a faint endotherm at 25°C because of a mesophase to isotropic transition. Polyurethane backbones of C8–C12OMeP have a high tendency to crystallise. Heated DSC scans of C*n*OMeP polyurethanes taken after annealing the samples at room temperature for seven days are shown in Fig. 3. The thermal properties of C6OMeP strongly depend on its thermal history. A DSC scan of the annealed C6OMeP exhibits an endothermic transition at 39°C ($\Delta H = 22.1\ \mathrm{J\,g^{-1}}$), which is attributed to the side chain melting. However, DSC scans of annealed C2–, C4–, C8–C12OMeP (Fig. 3) are the same as those carried out on the second heating (Fig. 2), indicating that their thermal properties are not highly sensitive to their thermal history as it is usually expected for polyurethanes because of their semicrystalline nature. The DSC scan of C8OMeP evidenced a faint exothermic peak at 65°C ($\Delta H = -4.1\ \mathrm{J\,g^{-1}}$) and two partially overlapping endothermic peaks at 89°C and 99°C ($\Delta H_{\mathrm{overall}} = 55.7\ \mathrm{J\,g^{-1}}$). The endothermic transition at 89°C is ascribed to the isotropisation of mesogenic units, while the transition at 99°C is attributed to the main chain melting. A DSC scan of C10OMeP exhibited an endothermic transition at 82°C ($\Delta H = 28.4\ \mathrm{J\,g^{-1}}$), which is related to the disappearance

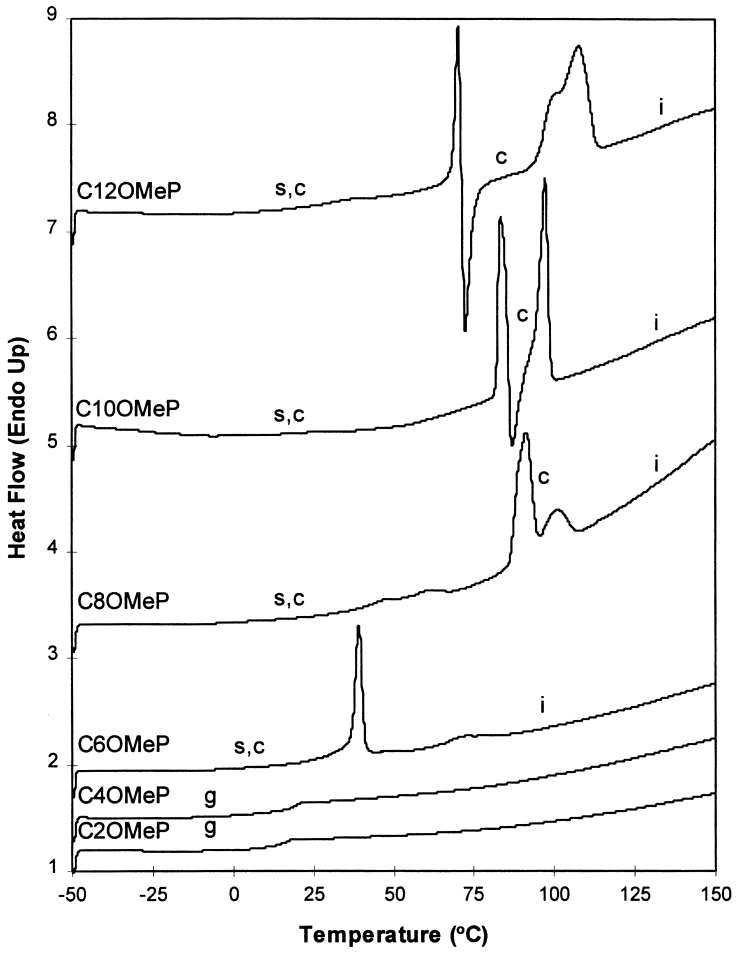

Fig. 3. The normalised heating DSC scans of C*n*OMeP polyurethanes taken after annealing the samples at room temperature for seven days: g – glassy phase, s – smectic phase, c – crystal phase, i – isotropic phase.

of the layer structure, cold crystallisation at 85°C ($\Delta H = -5.6$ J g^{-1}) and melting at 95°C ($\Delta H = 42.3$ J g^{-1}). Similar thermal behaviour was observed for C12OMeP, which exhibited an endothermic peak at 69°C ($\Delta H = 15.0$ J g^{-1}) followed by cold crystallisation at 71°C ($\Delta H = -22.1$ J g^{-1}) and main chain melting at 105°C ($\Delta H = 68.4$ J g^{-1}).

X-ray diffractograms of C2- and C4OMeP are consistent with their amorphous nature. They show a diffuse signal only with the maximum Bragg reflection at a periodicity of 4.3 Å, because of the disordered lateral arrangement of the mesogenic units (Fig. 4). In the small-angle region (Fig. 5), a diffractogram of C6OMeP has three Bragg reflections of the first, second and third order corresponding to the smectic layer spacing (d) 31.5 Å, which is 1.6 times the length of the fully extended mesogenic unit together with the spacer (trans-planar conformation) indicating the partially interdigitated bilayer structure of the smectic phase. In the wide-angle region, a diffuse signal at the periodicity of 4.3 Å and a sharp signal with the maximum Bragg reflection at the periodicity of 3.9 Å were observed (Fig. 4). The diffuse signal for the periodicity of 4.3 Å was ascribed to the lateral disorder of mesogenic units within smectic layers, while the sharp signal at the periodicity of 3.9 Å might be because of interchain distances of the side chains (side chain crystallisation). In the small-angle region, X-ray scattering curves of C8–C12OMeP polyurethanes consist of at least two sharp signals as a consequence of the lamellar structure. As can be seen in Fig. 5, for the C8OMeP Bragg reflections of the third and fourth order were observed, for C10OMeP Bragg reflections of the third, fourth and fifth order were observed, while for C12OMeP Bragg reflections were observed from the second to the fifth order. Pseudo-symmetry might be the reason why Bragg reflections of the first and second order were not detected. The main periodicities (smectic layer spacings (d)) of C8–C12OMeP calculated from higher order Bragg reflections are 35.2 Å for C8OMeP, 38.4 Å for C10OMeP and 40.8 Å for C12OMeP (Table 3). In the wide-angle region, diffractograms of C10- and C12OMeP have two strong sharp signals which are related to the high degree of order within smectic layers (Figs. 4 and 6). The maxima of Bragg reflections correspond to a periodicity of 5.0 and 3.7 Å respectively. The nature of the signal for the periodicity of 3.7 Å is not completely clear, it can be ascribed either to the two-dimensional lattice

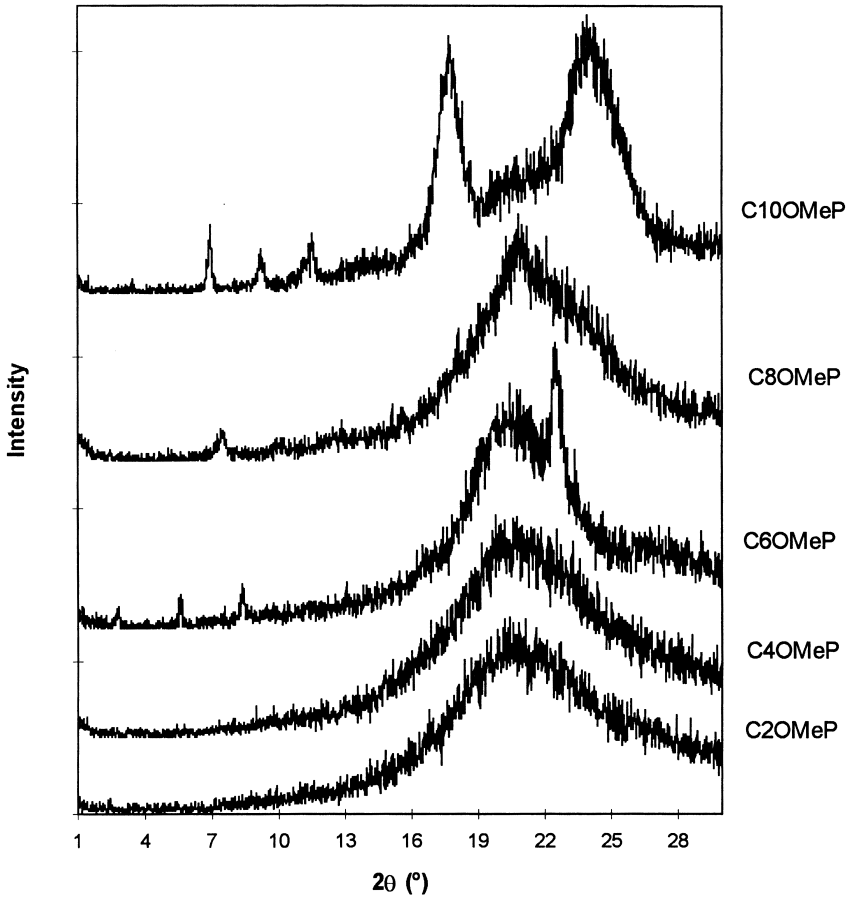

Fig. 4. X-ray diffractograms of C2–C10OMeP polyurethanes at room temperature.

in smectic layers (together with a signal at the periodicity of 5.0 Å) with a symmetry differing from a hexagonal one, or to the interchain distances of side chains (side chain crystallisation). Diffractograms of C12OMeP at different temperatures are shown in Fig. 6. The layer structure of C12OMeP, probably with the mesogens in an orthorhombic array within smectic layers, is stable up to 69°C. The disappearance of the layer structure was detected by a DSC as an

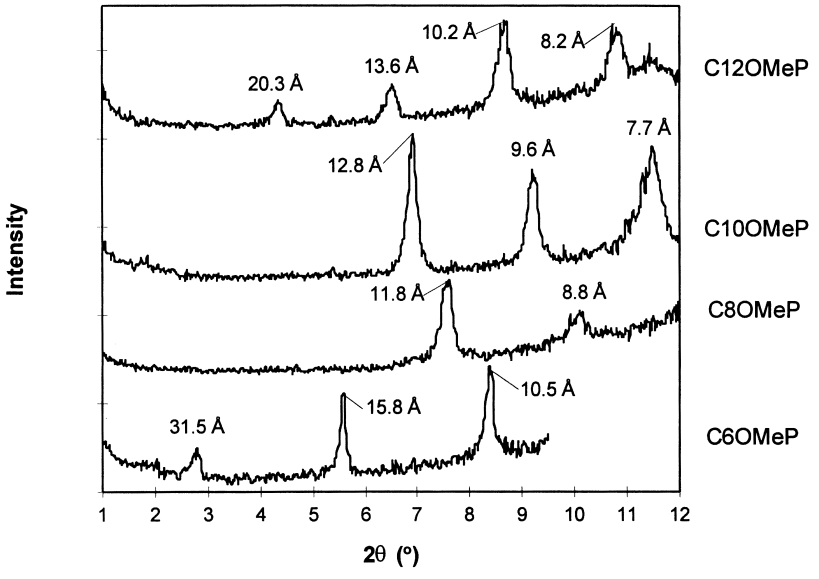

Fig. 5. X-ray diffractograms of C6–C12OMeP polyurethanes in small-angle region at room temperature.

Table 3
Layer spacings (d) obtained by means of small-angle X-ray diffraction and the theoretically calculated length (L) of fully extended mesogenic unit with spacer, the spacings of diffuse signals (d_d) in the wide-angle region and the interchain distances of side chains (d_{sc}), as well as the lateral spacings (d_{lat1}, d_{lat2}) of mesogenic units within the smectic layers for CnOMeP polyurethanes

	L (Å)	d (Å)	d_{lat1} (Å)	d_d (Å)	d_{sc}(Å)	d_{lat2} (Å)
C2OMeP	15.0			4.3		
C4OMeP	17.4			4.3		
C6OMeP	19.8	31.5		4.3	3.9	
C8OMeP	22.2	35.2		4.2		
C10OMeP	24.6	38.4	5.0			3.7
C12OmeP	26.3	40.8	5.0			3.7

endothermic transition at 69°C (Fig. 2). In the temperature range where the smectic phase is stable, the thickness of the smectic layers (40.8 Å) did not change with increasing temperature. Above 70°C, C12OMeP polyurethane shows a high degree of crystallisation (strong multiple reflections in wide-angle region, as shown in Fig. 6), which is closely related to hydrogen bonding between the polyurethane groups of the polyurethane backbone (Fig. 8). As can be seen in Figs. 2 and 6, the polyurethane backbone of C12OMeP melts above 100°C and shows rather unusual diffractograms with no reflections in the small-angle region and a sharp signal in the wide-angle region with the maximum Bragg reflection at a periodicity of 4.8 Å. This signal may be because of the hexagonal arrangements of mesogenic units, although without any order in the direction of their long axes. Freidzon et al. reported a similar X-ray diffraction pattern for a liquid crystalline polyacrylate. As the diffractogram did not correspond to any known liquid crystalline structure they suggested for it the new code letter N_B [18].

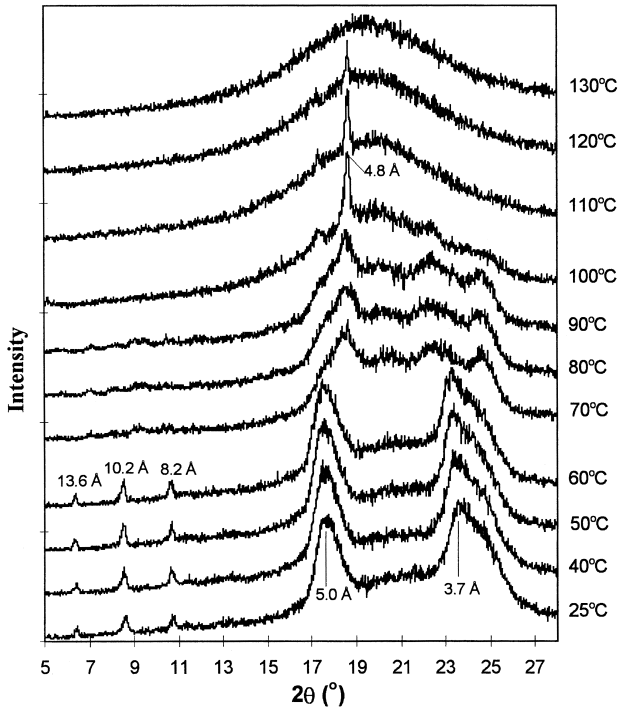

Fig. 6. X-ray diffractograms of C12OMeP polyurethane at different temperatures.

To establish the role of hydrogen bonding in mesophase formation, as well as crystallisation, Fourier transform infrared spectroscopy (FT-IR) studies of the synthesised polyurethanes were carried out at different temperatures focusing on the H-bonds between the N–H and C=O groups of the polyurethane backbone. IR spectra of CnOMeP differ in the N–H (3200–3500 cm^{-1}) and C=O (1600–1800 cm^{-1}) stretching regions as well as in the amide II region (1470–1570 cm^{-1}), as can be seen in Fig. 7. The dissociation of the H-bonds of the polyurethane groups for C2–C6OMeP took place evenly in the temperature range between 30°C and 150°C (Fig. 9). The frequency values of the band maxima of the C=O stretching vibrations of the above mentioned polyurethanes evenly shifted from approximately 1690 cm^{-1} at 30°C toward 1724 cm^{-1} at 150°C. The dissociation of the H-bonds of C8–C12OMeP is closely related to the melting of the polyurethane backbone. H-bond dissociation took place in the temperature range of main chain melting. For instance, for C12OMeP the frequency value of the band maxima of the C=O stretching vibration is almost constant (1688 cm^{-1}) in the temperature range between 30°C and 100°C (Figs. 8 and 9). Above 100°C in the narrow temperature range the frequency value of the band maximum jumped from 1689 cm^{-1} at 100°C to 1724 cm^{-1} at 120°C. This quick jump of the frequency value is accompanied by the endothermic transition detected by DSC measurements (Fig. 2). A comparison of DSC measurements, IR spectra and X-ray diffractograms at different temperatures, provides evidence that the backbone melting of CnOMeP is closely related to the dissociation of H-bonds between C=O and N–H groups, as can be seen in Fig. 9.

4. Conclusions

Hard segmented mesomorphic side chain polyurethenes (CnOMeP) with spacer lengths of 2, 4, 6, 8, 10 and 12 were synthesised by the addition polymerisation of α-[bis(2-hydroxyethyl)amino]-ω-(4-methoxyazobenzene-4′-oxy)alkanes (CnOMe-diol) with hexamethylene diisocyanate. Their mesomorphic behaviour was examined by means of POM, differential scanning calorimetry and X-ray diffraction. The spacer length plays an important role in the thermal behaviour of CnOMeP not only in that it influences mesophase formation but also in that it determines the degree of crystallisation as well. C2- and C4OMeP were amorphous while those with longer spacers had a high tendency toward crystallisation, which was found to be kinetically controlled, especially for C6OMeP. For C6–C12OMeP polyurethanes, bilayer smectic structures with

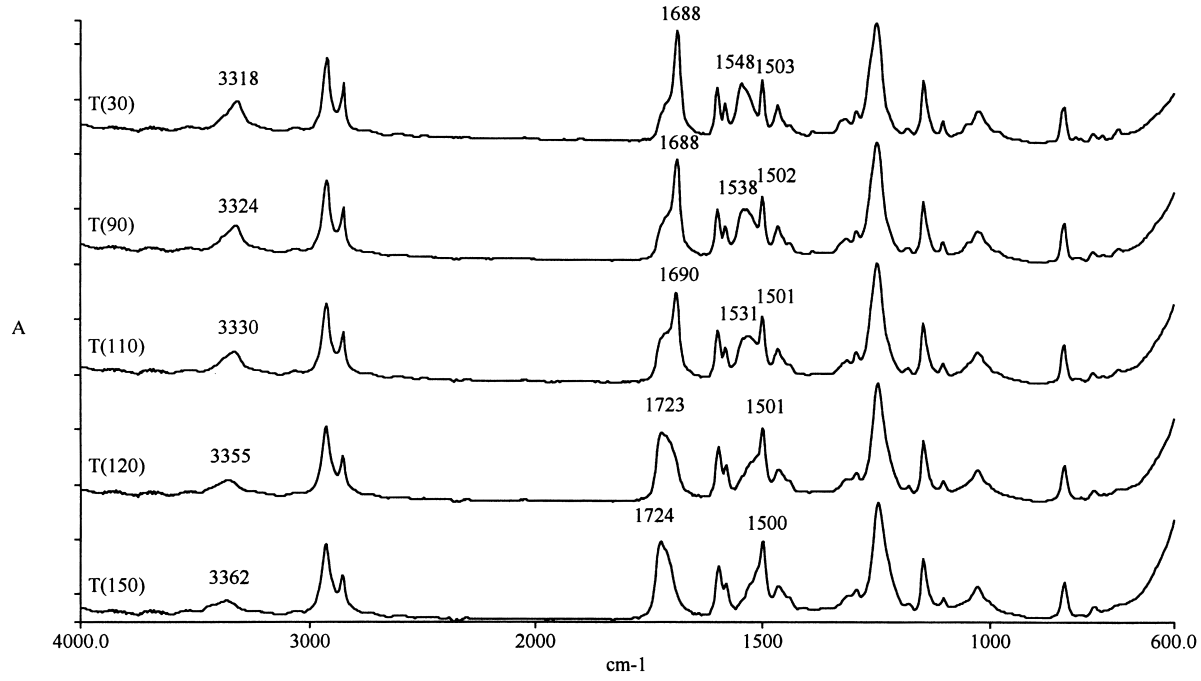

Fig. 7. IR spectra of C12OMeP polyurethane at different temperatures *T*(°C).

layer spacings ranging from 31.5 Å for C6OMeP to 40.8 Å for C12OMeP were found.

A careful examination of the FTIR spectra of C*n*OMeP in the C=O stretching (1600–1800 cm^{-1}) and N–H stretching (3200–3500 cm^{-1}) regions recorded as a function of increasing and decreasing temperature, together with DSC measurements, revealed the close connections between the main chain melting and H-bonds dissociation of C*n*OMeP. Not only the temperature dependence but also the influence of the spacer length on the formation of H-bonds was found. The dissociation of the H-bonds of the polyurethane groups for C2–C6OMeP took place evenly with increasing temperature, while C8–C12OMeP behaved differently. The frequency values of the band maxima of the C=O stretching vibrations

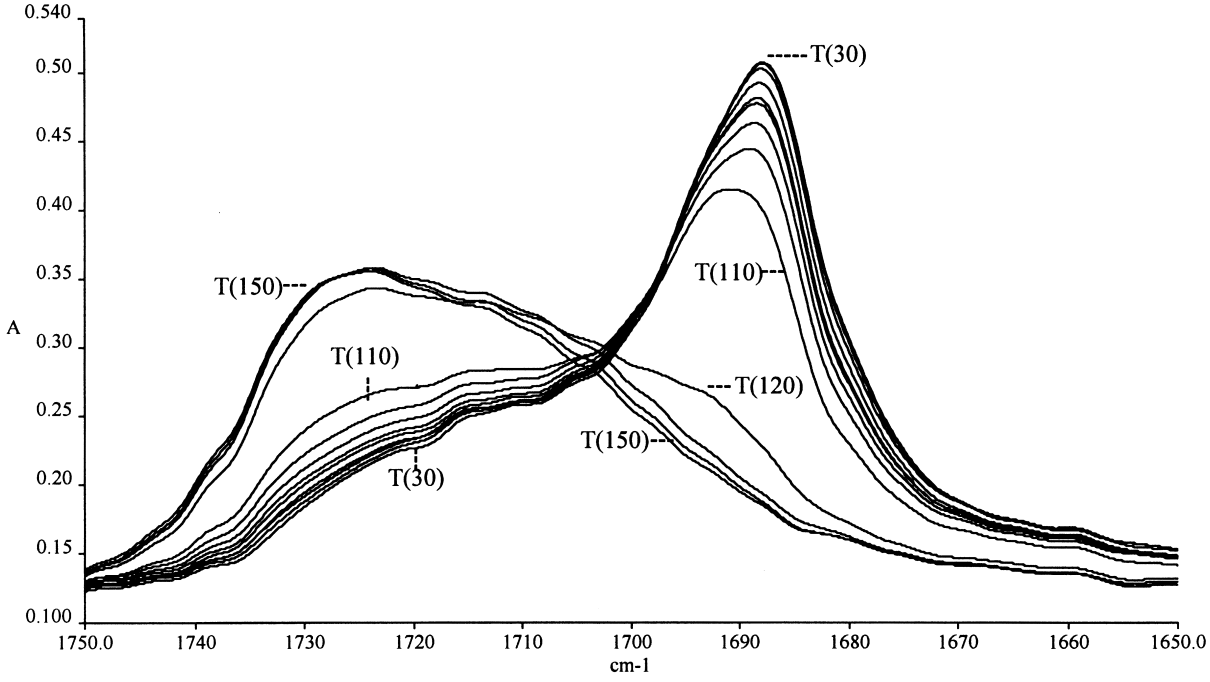

Fig. 8. IR spectra of C12OMeP polyurethane in the C=O stretching region recorded as a function of increasing temperature *T*(°C) in the temperature range between 30°C and 150°C.

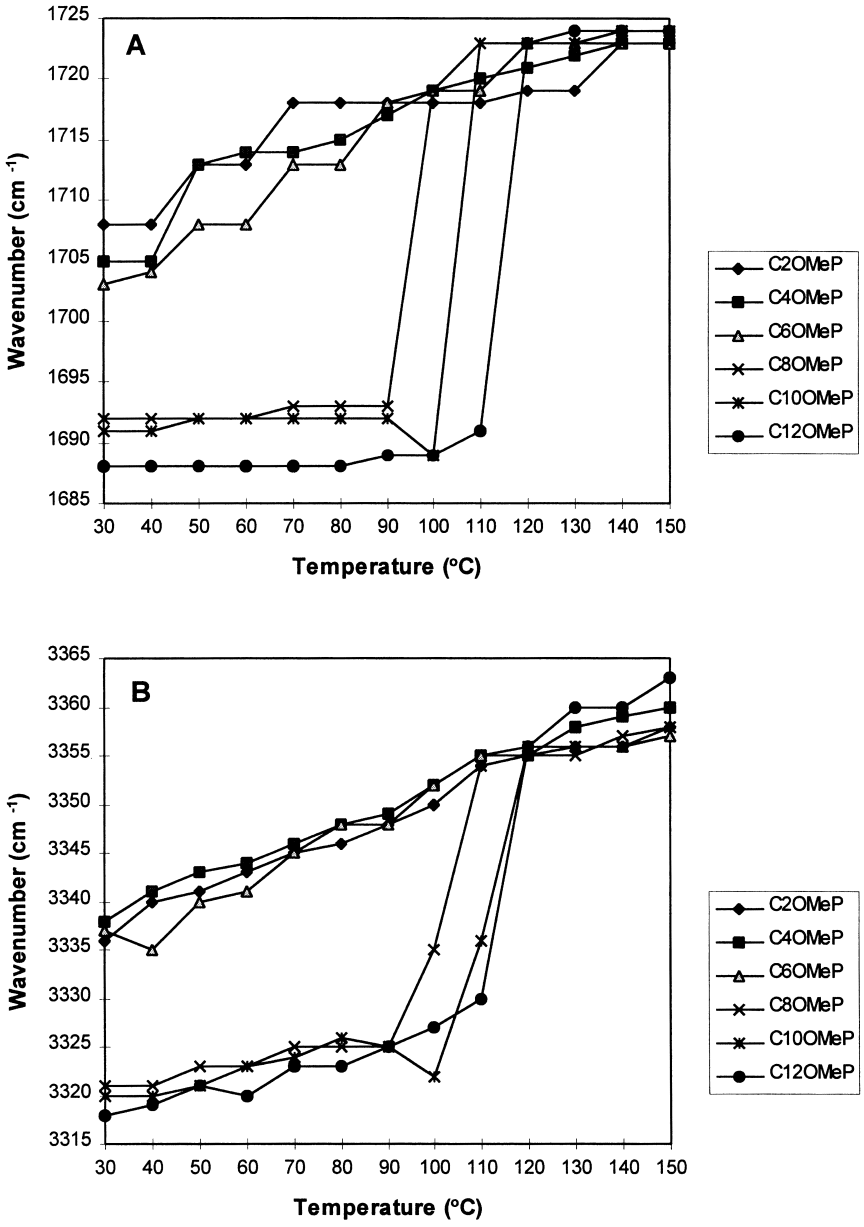

Fig. 9. Shifts of the band maxima of C*n*OMeP polyurethanes: A – for the C=O stretching vibration, B – for the N–H stretching vibration as a function of temperature.

of C2–C6OMeP evenly shifted from approximately 1690 cm^{-1} at 30°C toward 1724 cm^{-1} at 150°C. For C8–C12OMeP, H-bond dissociation took place in the temperature range of main chain melting. For instance, for C12OMeP the frequency value of the band maxima of the C=O stretching vibration is around 1688 cm^{-1} in the temperature range between 30°C and 100°C. Subsequently, in the narrow temperature range the frequency value of the band maximum jumped from 1689 cm^{-1} at 100°C to 1724 cm^{-1} at 120°C. This quick jump of the frequency value is accompanied by an endothermic peak as detected by DSC measurements indicating that the backbone melting of C12OMeP polyurethane is closely related to the dissociation of H-bonds between C=O and N–H groups.

Acknowledgements

This work is a part of the project J2-7505. The authors would like to thank the Ministry of Science and Technology of the Republic of Slovenia for financial support. We thank Dr. Tone Meden for the beneficial discussions as well.

References

[1] Trollsas M, Sahlen F, Gedde UW, Hult A, Hermann D, Rudquist P, Komitov L, Lagerwall ST, Stebler B, Lindstrom J, Rydlund O. Macromolecules 1996;29:2590.
[2] Reinhardt BA. TRIP 1993;1:4.

[3] Meng X, Natansohn A, Barrett C, Rochon P. Macromolecules 1996;29:946.
[4] Craig AA, Imrie CT. J Polym Sci A Polym Chem 1996;34:421.
[5] Craig AA, Imrie CT. J Mater Chem 1994;4:1705.
[6] Percec V, Tomazos D, Willingham RA. Polym Bull 1989;22:199.
[7] Graig AA, Imrie CT. Macromolecules 1995;28:3617.
[8] Stevens H, Rehage G, Finkelmann H. Macromolecules 1984;17: 851.
[9] Percec V, Keller A. Macromolecules 1990;23:4347.
[10] Imrie CT, Karasz FE, Attard GS. Macromolecules 1993;26:3803.
[11] Collings PJ, Hird M. Introduction to liquid crystals; chemistry and physics. London: Taylor and Francis, 1997 p. 93.
[12] Percec V, Pugh C. Molecular engineering of predominantly hydrocarbon-based LCPs. In: McArdle CB, editor. Side chain liquid crystal polymers. Glasgow: Blackie, 1989. p. 30.
[13] Simmonds DJ. Thermotropic side chain liquid crystal polymers. In: Collyer AA, editor. Liquid crystal polymers: from structures to applications. Amsterdam: Elsevier, 1992. p. 349.
[14] Mirčeva A, Oman N, Žigon M. Polym Bull 1998;40:469.
[15] Brecl M, Malavašič T. J Polym Sci A: Polym Chem 1997;35:2871.
[16] Brecl M, Žigon M, Malavašič T. J Polym Sci A: Polym Chem 1998;36:2135.
[17] Brecl M, Malavašič T. Kov Zlit Tehnol 1996;30:83.
[18] Noël C. Macroscopic structural characterization of side chain liquid crystal polymers. In: McArdle CB, editor. Side chain liquid crystal polymers. Glasgow: Blackie, 1989. p. 159.